

SiO₂ seems to suggest that interface states were generated by breaking the strained bonds at the Si-SiO₂ interface. This mechanism, suggested by Gwyn¹¹, was used by Ma *et al.*^{12,13} to interpret the generation of interface states in an electron-irradiated MOS capacitor very consistently. Another possible mechanism as described by Nicollian *et al.*¹⁴ is that a moisture-related center near the Si-SiO₂ interface might capture an emitted electron which breaks the bond between the hydrogen and the center, permitting hydrogen to escape; and an interface state is hence created. It should be mentioned that the interface states can also be created by hole transport through the Si-SiO₂ interface as reported by Powell *et al.*¹⁵ and Winokur *et al.*¹⁶ The breaking of strained bonds at the interface by the transporting holes is also one of the suggested possible mechanisms.¹⁶ Further experiments on samples processed with different moisture content and annealing ambients would provide better indications as to which one is the favorable mechanism during the emission of leakage electrons.

As discussed by Ning *et al.*,⁷ leakage electrons, both generation and diffusion components, can be emitted only when they gain enough energy from the electric field in the depletion region to surmount the Si-SiO₂ interface barrier; hence, the emission current is a strong function of temperature and substrate-diffusion bias, as is the generation of interface states as shown in Fig. 1. When substrate bias decreased from -10 to -15 V, the rate of interface state generation increased significantly. Consequently, experiments carried out on differently processed samples and stressed at various temperatures and substrate biases would give us more insight of interface state generation.

In conclusion, we have clearly demonstrated that interface states are generated due to the emission of

leakage electrons from the silicon substrate into SiO₂ by the high-frequency and quasistatic C-V technique. These interface states can mostly be annealed out at 200 °C. Since interface states can cause device degradation, they could be a serious reliability concern, especially at high operating temperatures where the leakage current level is high.

The author would like to thank Dr. T. P. Ma for helpful discussions and for supplying the computer program for calculating the interface-state distribution and C. E. Lucas for experimental assistance.

*Present address: IBM T.J. Watson Research Center, Yorktown Heights, N.Y. 10598.

¹B. A. McDonald, IEEE Trans. Electron Devices ED-17, 871 (1970).

²J. F. Verwey, Appl. Phys. Lett. 15, 270 (1969).

³J. F. Verwey and B. J. DeMaagt, IEEE Trans. Electron Devices ED-19, 245 (1972).

⁴Y. T. Yeow, D. R. Lamb, and S. D. Brotherton, J. Phys. D 8, 1495 (1975).

⁵E. H. Nicollian and A. Goetzberger, Proc. 6th Annual Reliability Phys. Symp., 1967, p. 66 (unpublished).

⁶E. H. Nicollian and C. N. Berglund, J. Appl. Phys. 41, 3052 (1970).

⁷T. H. Ning, C. M. Osburn, and H. N. Yu, Appl. Phys. Lett. 29, 198 (1976).

⁸M. Kuhn, Solid-State Electron. 13, 873 (1970).

⁹P. V. Gray and D. M. Brown, Appl. Phys. Lett. 8, 31 (1966).

¹⁰G. A. Scoggan and T. P. Ma, J. Appl. Phys. 48, 294 (1977).

¹¹C. W. Gwyn, J. Appl. Phys. 40, 4886 (1969).

¹²T. P. Ma, G. Scoggan, and R. Leone, Appl. Phys. Lett. 27, 61 (1975).

¹³T. P. Ma, Appl. Phys. Lett. 27, 615 (1975).

¹⁴E. H. Nicollian, C. N. Berglund, P. F. Schmidt, and J. M. Andrews, J. Appl. Phys. 42, 5654 (1971).

¹⁵R. J. Powell and G. F. Derbenwick, IEEE Trans. Nucl. Sci. NS-18, 99 (1971).

¹⁶P. J. Winokur and M. M. Sokolowski, Appl. Phys. Lett. 28, 627 (1976).

Barrier-controlled low-threshold *pnpn* GaAs heterostructure laser*

C. P. Lee, A. Gover, S. Margalit, I. Samid, and A. Yariv

California Institute of Technology, Pasadena, California 91125

(Received 1 November 1976; accepted for publication 11 March 1977)

Incorporation of GaAlAs potential barrier layers into the active regions of a heterostructure *pnpn* injection laser makes it possible to design Shockley diode lasers with low (3 kA/cm²) room-temperature threshold currents.

PACS numbers: 42.55.Px, 73.40.Lq, 85.30.De

A *pnpn* diode¹ displays negative resistance characteristics which cause it to switch from a low-current-high-voltage state to one of high current and low voltage once the terminal voltage exceeds the breakover voltage V_{BO} as shown in Fig. 1.

Previous work resulted in the demonstration of homostructure² and heterostructure³ *pnpn* lasers which, however, required high threshold currents.

The high threshold current of the previous devices was due to the fact that the optical and electrical requirements were in contradiction. To obtain a high "on" current following switching (see Fig. 1) one requires a device with a large V_{BO} . This can be accomplished by reducing the emitter injection efficiency at the emitter-base junctions³ or by using large "base" regions to reduce the minority-carrier base transport factor. Both of these solutions, however, increase the laser

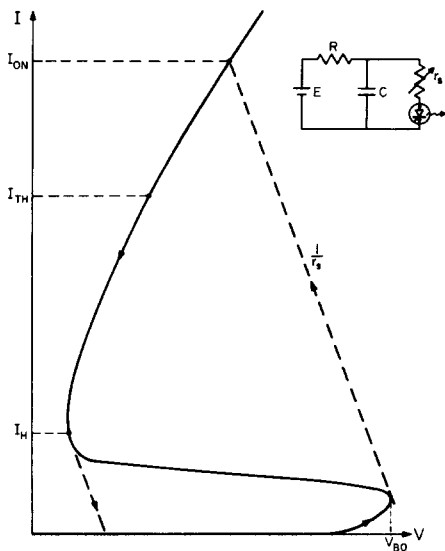


FIG. 1. The I - V characteristic of a $pnpn$ laser diode and the dynamic load line trace in an oscillating circuit connection.

threshold current density. The increase in threshold is due to the fact that the base regions are also the active regions of the lasers so that increasing their widths leads to a reduced gain. The reduction in the injection efficiency leads in an obvious way to a smaller density—at a given total current—of injected minority carriers in the base regions (layers 3 and 6) and thus to a smaller laser gain.

In the present work we describe a solution to this problem which resulted in an order-of-magnitude reduction of the lasing threshold current density. We have reduced the base transport factors by using heteroepitaxy to introduce GaAlAs potential barriers into the base regions. These barriers are marked by ΔE in Fig. 2. The barrier also helped to alleviate the punch-through effect. These enabled us to obtain a high breakover voltage V_{BO} , and consequently a high "on" current I_{ON} , while preserving the small width of the base regions and a high injection efficiency. The resulting laser oscillated at a threshold current density of 3 kA/cm^2 .

Figure 2 shows the layer sequence and composition as well as a band diagram of the device in the blocking state where junction J_{45} (the junction between layers 4 and 5) is reverse biased. Carriers which are injected from the emitters (layers 2 and 7) are impeded by the potential barriers (layers 4 and 5) which cause most of the carriers to recombine in the GaAs bases (layers 3 and 6). The remaining carriers cross the barriers to the "collectors" regions (layers 5 and 4). If we use the equivalent two-transistor model¹ to describe the $pnpn$ diode then we can explain the effect of the base GaAlAs barriers ΔE as causing a reduction in the transistors' gain.

Referring to Fig. 2, the gain β_1 of the $nnpn$ transistor with a GaAs base of width w_3 is reduced by a barrier layer of width w_4 and a height ΔE to a value β_2 where

$$\frac{\beta_1}{\beta_2} = 1 + \left(\frac{w_4}{w_3}\right)^2 + 2\left(\frac{w_4}{w_3}\right) \exp\left(\frac{\Delta E}{kT}\right). \quad (1)$$

Equation (1) is an approximation valid in the limit when the diffusion length is small compared to the base width.⁴ In the GaAs-Ga_{1-x}Al_xAs system $\Delta E/kT \sim 50x$ so that a very small change in the aluminum concentration x causes very large variations in β .

In the ON condition the voltage across the central junction J_{45} (see Fig. 2) drops until the junction is slightly forward biased. The structure then operates as a heterostructure laser with two active regions. Majority carriers are injected efficiently from layers 2 and 7 and most of the recombination takes place in the low-band-gap active regions (layers 3 and 6). The small widths (w_3 and w_6) of the active regions lead to a low lasing threshold current. We have measured $J_{th} = 3 \text{ kA/cm}^2$ at room temperature, which is comparable to our conventional heterostructure lasers with the same active region thickness.

The devices were fabricated by conventional horizontal liquid-phase-epitaxial growth techniques. The epitaxial layers were grown on a (100)-oriented $n = 3 \times 10^{18} \text{ cm}^{-3}$ GaAs substrate. The external layers (2, 7, and 8) were doped in excess of 10^{18} cm^{-3} . The internal layers (3–6) were doped to less than $5 \times 10^{16} \text{ cm}^{-3}$. After growth, the substrate was lapped down to $100 \mu\text{m}$ thickness and Ohmic contacts were applied to the top layer and to the substrate. The slice was then cleaved and sawed and the laser chips mounted on TO-5 transistor headers.

The design parameters—layer widths and barrier heights—were varied from growth to growth in order to investigate their effect on the device switching and lasing characteristics. We have fabricated three types of devices: (1) with double potential barrier (Fig. 2), (2) with single barrier in the p base ($w_5 = 0$), and (3) with no barriers ($w_4 = w_5 = 0$). The effect of additional and higher barriers was to decrease the gain of the internal transistors. An increase of the bases' widths had a similar effect. As would be expected¹ the breakover voltage V_{BO} and the holding current I_H increased as the gain of the internal transistors decreased. How-

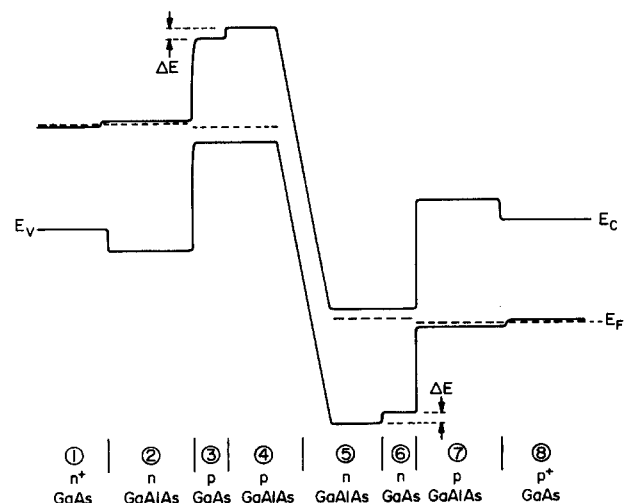


FIG. 2. The energy diagram of a double-barrier $pnpn$ heterostructure laser in the blocking (OFF) state.

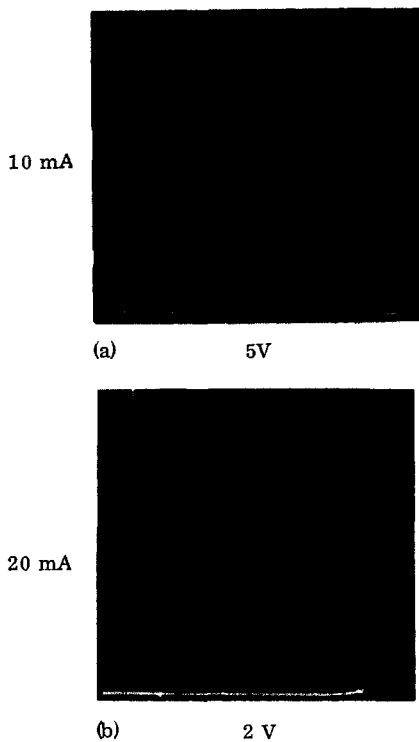


FIG. 3. The I - V characteristics of two different diodes: (a) single-barrier wide-base diode; (b) double-barrier thin-base diode.

ever, when one of the transistor bases was too thin, low V_{BO} values were found even in low-gain structures because of the *punch-through* effect. The measured lasing threshold current density decreased with the widths of the active regions (layers 3 and 6).

Figure 3 shows the I - V characteristic oscillograms of two different diodes. Figure 3(a) corresponds to a single-barrier device at interface 3-4 with wide bases ($w_3 = 2.4 \mu\text{m}$, $w_4 = 2.1 \mu\text{m}$, $w_5 = 0$, $w_6 = 3.5 \mu\text{m}$, Al concentration in barrier $x = 0.2$), while Fig. 3(b) corresponds to a double-barrier device with narrow bases ($w_3 = 0.4 \mu\text{m}$, $w_4 = w_5 = 1.5 \mu\text{m}$, $w_6 = 0.4 \mu\text{m}$, $x = 0.15$). The first structure possesses a high breakover voltage ($V_{BO} \approx 47 \text{ V}$). The second structure has lower breakover voltage ($V_{BO} \approx 17 \text{ V}$) caused, probably, by punch-through. However, the narrow active regions of the second structure permitted low lasing threshold ($J_{th} \approx 3 \text{ kA/cm}^2$ at room temperature), while no lasing was observed with the first structure.

The devices were operated in a (current) relaxation oscillation mode using the circuit arrangement shown in Fig. 1. Figure 4 shows oscillograms of the current and light output of the double-barrier device whose I - V curve trace is shown in Fig. 3(b). The circuit was operated with a bias voltage of 25 V, a charging resistor $R = 420 \Omega$, and a capacitor $C = 0.2 \mu\text{F}$. The current pulse level was changed by adjusting the 10- Ω trimpot resistor r_3 . The lasing threshold current of this device was $I_{th} \approx 3.3 \text{ A}$. Note that as the current increases from below threshold [Fig. 4(a)] to above threshold [Fig. 4(b)] the light pulse (measured from an S1 photomultiplier) increases in a nonlinear way and also narrows! A plot

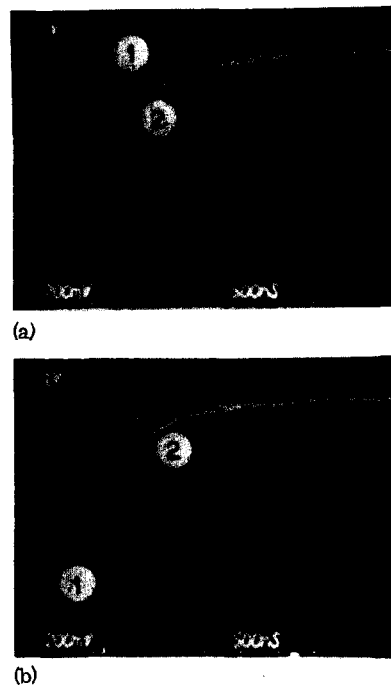


FIG. 4. The current and light output oscilloscope traces of a *pnpn* laser connected in the electronic circuit shown in Fig. 1. (a) Below threshold: 1—light pulse, 2—current pulse; (b) above threshold: note the narrowing and nonlinear increase of the lasing light pulse relative to the current pulse.

of the device emission spectrum 10% above threshold is shown in Fig. 5.

In conclusion, the incorporation of potential barriers into the active regions of *pnpn* heterostructure lasers provides a new type of control over the switching and lasing characteristics of the device. It thus makes possible a simultaneous low lasing threshold current (I_{th}) and a high breakover voltage (V_{BO}) and ON condition current (I_{on}). It is suggested that this device may be useful in pulse code modulation and pulse position modulation optical communication, and in high-temperature electronic SCR applications.

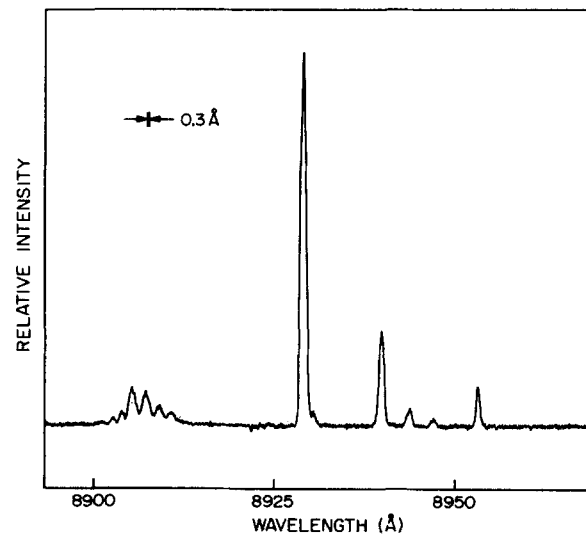


FIG. 5. Lasing spectrum of a room-temperature-operated *pnpn* laser.

*Research supported by the Office of Naval Research and the National Science Foundation.

¹S. M. Sze, *Physics of Semiconductor Devices* (Wiley-Interscience, New York, 1974).

²W. F. Kosonocky, R. H. Cornely, and I. G. Heggi, *IEEE J. Quantum Electron.* QE-4, 176-179 (1968); Yu. P. Demidov,

M. N. Zargar'yants, A. A. Kiselev, and S. I. Kolonekova, *JETP Lett.* 12, 117 (1970).

³H. F. Lockwood, K. F. Etzold, T. E. Stockton, and D. P. Marinelli, *IEEE J. Quantum Electron.* QE-10, 567 (1974).

⁴A. Gover, S. Margalit, C. P. Lee, I. Samid, and A. Yariv (unpublished).

Lateral current confinement by reverse-biased junctions in GaAs-Al_xGa_{1-x}As DH lasers

W. T. Tsang and R. A. Logan

Bell Laboratories, Murray Hill, New Jersey 07974

(Received 17 December 1976; accepted for publication 18 March 1977)

Two methods are described for fabrication of a DH stripe-geometry laser where lateral current confinement is obtained with reverse-biased junctions on both sides of the active layer. Threshold current densities, comparable in values to optimum values achieved in other stripe geometry lasers, are obtained as a function of top channel widths for lasers with single and double current confinement. The lasers exhibit clean stable mode patterns with excellent linearity of the optical output power as a function of injection current. Lasers with channel widths $\leq 14 \mu\text{m}$ operate in the lowest-order transverse mode in the junction plane for currents up to \sim two times the threshold (an output power of 16 mW per mirror).

PACS numbers: 42.55.Px, 42.80.Sa, 73.40.Lq

A variety of stripe-geometry double-heterostructure (DH) GaAs-Al_xGa_{1-x}As lasers¹ have been developed to minimize the current threshold for room-temperature cw operation. In these lasers, the current injection is laterally confined to a narrow stripe (~ 5 – $\sim 30 \mu\text{m}$) by one of the following techniques: oxide masking,² mesa etching,³ proton bombardment,⁴ etched-buried technique,^{5–7} stripe-embedding technique,⁸ single *p-n* junction stripe technique,⁹ and diffusion isolation which includes planar stripe,¹⁰ junction stripe,¹¹ internal stripe,¹² and substrate-stripe geometries.¹³

In this paper, we report a novel current injection confinement technique in conventional DH lasers that is shown schematically in cross section in Fig. 1, where the layer compositions and dimensions are listed. When the diode is forward biased (top contact positive) the *n-p* junctions demarcated by -x-x-x- are reverse biased and lead to current flow only through the two superimposed top and bottom windows. With this double lateral injection current confinement (DCC), the lateral spreading of current¹⁴ through the laser is expected to be reduced as compared to that of some of the single lateral injection current confinement (SCC) schemes listed above.^{5,9,11,13} The DCC assists the restriction of current flow through the laser so that at a given level of total injection current, the current density at the active layer is increased with resulting reduction in laser current threshold.

The DCC lasers have been fabricated by LPE in two different ways. In the first method, using two LPE growths [Fig. 1(a)], a *p*-GaAs layer was first grown on a (100)-oriented *n*-GaAs substrate by LPE. Then using narrow stripe windows, ranging in width from ~ 10 to $\sim 30 \mu\text{m}$, in AZ1350 photoresist as a mask, channels

were etched through the *p*-GaAs epilayer into the *n*-GaAs substrate using $\text{H}_2\text{SO}_4 : \text{H}_2\text{O}_2(30\%) : \text{H}_2\text{O} = 1 : 8 : 10$ at 24 °C. After stripping off the photoresist mask, the sample was then cleaned by etching for a few seconds in dilute Br-methanol and the conventional DH laser structure with an additional top *n*-Ga_{0.55}Al_{0.45}As layer was grown by LPE. Since this growth is entirely on a GaAs substrate, no wetting problems are encountered. In the second method, using a single LPE growth cycle [Fig. 1(b)] the (001) GaAs seed crystal was preprocessed so as to form a parallel series of stripe mesas, using the masking and etching procedures described above. The mesas were $\sim 5 \mu\text{m}$ high, with widths ranging from ~ 10 to $\sim 30 \mu\text{m}$, and oriented along the $[\bar{1}10]$ direction. The DCC laser structure was then formed in a single LPE growth, with the epitaxial layers grown in the sequence shown in Fig. 1(b). The first *p*-Ga_{0.78}Al_{0.22}As layer which forms the lower current confining junction does not grow on the top of the mesa, where nucleation is apparently inhibited, so that windows, with widths defined by the mesas, automatically formed in the lower *n-p* junction as shown in Fig. 1(b). This growth nucleation phenomena has also been observed in the formation of buried heterostructures.^{5,15}

In both procedures, after the epilayer growth, anodically grown native oxide¹⁶ was then used as an etching mask to form identical windows over the first set of windows by realignment of the same photoresist mask. The exposed Ga_{0.55}Al_{0.45}As was then etched selectively down to the *p*-GaAs layer using an iodine etch (113 g KI, 65 g I₂, 100 cm³ H₂O). Conventional contacts were then metalized on both surfaces. Finally, individual laser diodes were formed by the usual cleaving procedures.